academicJournals

Vol. 8(16), pp. 699-706, 30 April, 2013
DOI: 10.5897/IJPS2013.3872
ISSN 1992-1950 © 2013 Academic Journals
http://www.academicjournals.org/IJPS

International Journal of Physical Sciences

Full Length Research Paper

Widely tunable micro electromechanical systems (MEMS)-vertical-cavity surface-emitting lasers with single transverse mode operation

Seyed Mahdi Hatamian[1]*, Vahid Ahmadi[2] and Elham Darabi[3]

[1]Department of Electrical Engineering, Science and Research Branch, Islamic Azad University, Tehran, Iran.
[2]Department of Electrical Engineering, Tarbiat Modares University, Tehran, Iran.
[3]Plasma Physics Research Center, Science and Research Branch, Islamic Azad University, Tehran, Iran.

Accepted 8 April, 2013

In this paper, a micro electromechanical systems vertical-cavity surface-emitting laser (MEMS-VCSEL) with asymmetric double oxide aperture and highly strained GaInNAsSb quantum wells for widely tunable, single mode and high temperature operation has been investigated. The MEMS-VCSEL is based on an integrated two-chip concept which allows us to extend the single wavelength performance to a continuously tunable, selectively wavelength-addressable spectrum of 40 nm. It has a much larger tuning range as compared with previous works. We present a comprehensive model including electrostatic membrane equation coupled with thermal, spatial and temporal rate equations considering Shockley Read Hall (SRH), Auger and carrier diffusion effects. These coupled equations are solved numerically by finite difference method (FDM). Using the simulation results, we design a single mode, high power, high temperature and tunable VCSEL, which is suitable for C-band dense-wavelength-division- multiplexing (DWDM) optical communication systems.

Key words: Micro electromechanical systems (MEMS), tunable vertical-cavity surface-emitting laser (VCSELs), strained GaInNAsSb QWs, single mode operation.

INTRODUCTION

Tunable, single mode and high power vertical-cavity surface-emitting laser (VCSELs) at 1550 nm have a great potential to replace the distributed feedback (DFB) and fabry-perot (FP) edge emitting lasers that are currently used in optical communication (Kogel et al., 2011). Low threshold current together with easily couple light into optical fiber is possible due to their small active volume compare to edge-emitting lasers. Recently many structures of micro electromechanical systems vertical-cavity surface-emitting laser (MEMS-VCSELs) have been reported. These devices can be divided into three categories: cantilever VCSELs (Chang-Hasnain, 2000), membrane VCSEL devices (Guan et al., 2009), and tunable VCSELs utilizing a half-symmetric cavity (Tayebati et al., 1999).

For tuning in cantilever VCSELs, the technique is based on changing the cavity length using cantilever arm and in half-symmetric cavity VCSELs; the curved top mirror is designed to match the Gaussian curvature of the light oscillating within the optical cavity that creates a single spatial lasing mode. We are primarily concerned with VCSEL tuning utilizing electrostatically actuated membrane with minimum actuation voltages which is comparable to existing MEM tunable VCSEL structures.

*Corresponding author. E-mail: m.hatamian@srbiau.ac.ir. Tel/Fax +982188113311.

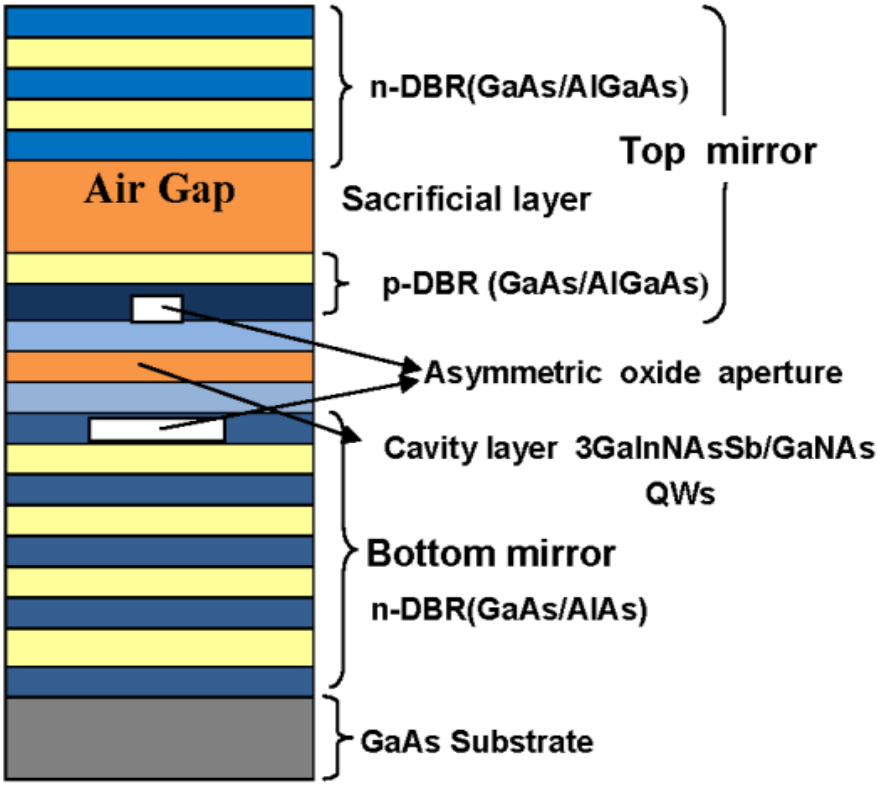

Figure 1. The schematic structure of the proposed MEMS-VCSEL.

In surface micro machined material layers are deposited and patterned one at a time and it is possible to create membrane VCSELs. Many approaches to achieve single mode, high temperature, and high power operations have been reported (Zhou and Mawst, 2002). There are different effects such as pump induced current spreading, spatial hole burning and thermal gradients inside the cavity on the carrier distribution which lead to VCSELs multi mode behaviour (Samal et al., 2005; Nakwaski and Sarzala, 1998). Our aim is to optimize a tunable VCSEL based on the GaAs material system with dilute nitride/antimonide quantum wells for the long wavelength. To resolve the issue of multi-mode behavior, a new structure design using asymmetric double apertures is proposed and theoretically modeled. Here an electrostatic tunable 1.55 μm MEMS-VCSEL based on two-chip concept with a tuning range more than 40 nm is proposed and single mode operation is achieved by engineering the spatial distribution of the injection current profile using asymmetric oxide apertures.

Using finite difference method (FDM), the device performance by solving a comprehensive model has been investigated. It includes electrostatic membrane equation coupled with thermal, spatial and temporal rate equations considering Shockley Read Hall (SRH), Auger and carrier diffusion effects. Base on the simulation results, we design a widely tunable, single mode, high power and high temperature VCSEL appropriate for dense-wavelength-division-multiplexing (DWDM) optical communication system.

TWO-CHIP MEMS-VCSEL DESIGN

The proposed device consists of a bottom n-DBR, a cavity layer and a top mirror as shown in Figure 1. GaAs substrate based materials are the excellent choice for long-wavelength operation due to better thermal performance (Martin, 2001). The bottom stack consists of 22.5 pairs n-doped GaAs/AlAs DBR which is perfectly lattice matched to GaAs substrate. The active region consists of three highly strained $Ga_{0.59}In_{0.41}N_{0.028}As_{0.942}Sb_{0.03}$/GaNAs QW for long-wave applications (Gutowski and Sazala, 2008).

GaInNAsSb/GaNAs lasers have excellent high-temperature performance, large T_0, greater efficiency and higher output power. The QWs are sandwiched by two stacks of λ/4 brag mirrors for 1.55 μm. The 100 × 100 μm top mirror, includes three parts: a p-DBR, an air gap, and a top n-DBR, which is freely suspended above the laser cavity and supported via a membrane structure. The p-DBR consists of 4 pairs GaAs/$Al_{0.9}Ga_{0.1}$As. The air gap,

Table 1. Device parameters.

Element	Material	Thickness	Refractive Index	Comment
MEMS DBR	AlGaAs/GaAs	5 µm	3.38/2.99	λ/4
Air-gap	AlGaAs	1.4 µm	1.0	Sacrificial layer
QW and barriers	GaInNAsSb /GaNAs	7/20 (nm)	3.6/3.5	3QWs
Bottom DBR	GaAs/AlAs	5.5 µm	3.53/2.97	λ/4

followed by a section of n- DBR consists of 20.5 pairs GaAs/AlGaAs. Also a double asymmetric aperture VCSEL is proposed when p-aperture is at the third pair in p-DBR and n-aperture at the first pair in bottom n-DBR. The DBR mirrors are doped with Be and Si. Be ($N_{Be} = 5 \times 10^{17}$ cm^{-3} for GaAs, $N_{Be} = 2 \times 10^{18}$ cm^{-3} for AlGaAs) is used as p-dopant, where as Si ($N_{Si} = 5.3 \times 10^{17}$ cm^{-3} for GaAs, $N_{Si} = 3 \times 10^{18}$ cm^{-3} for AlAs) is used as the n-dopant. The topest layer is heavily doped with Be ($N_{Be} = 6 \times 10^{19}$ cm^{-3}) for facilitate current spreading and ohmic contact. The device parameters are summarized in Table 1.

THEORY OF ANALYSIS

Electrostatic equations

Wavelength tuning is accomplished by applying a voltage between the top n-DBR and p-DBR, across the air gap. A reverse bias voltage is used to provide the electro static force, which deflects the membrane downward and shortens the air gap, thus shifts the laser wavelength to shorter wavelengths (blue shift) (Ochoa, 2007). The displacement of the membrane is controlled by the balance between the electrostatic force and the elastic restoring force in membrane legs which is described by the second-order linear differential equation as (Ochoa, 2007):

$$\frac{d^2y}{dx^2} = \frac{M(x)}{EI} \tag{1}$$

Where E is Young's modulus (Pa), and I is the moment of inertia (m^4). *EI* product is known as the flexural rigidity of the beam. *M(x)* represents the bending moment ($N.m^2$).

Here L, t and w are flexure's length, thickness and width, respectively. For small deflections, the electrostatic force obeys the Hook's law ($F=k_{total}\, d$), so for 4 flexures:

$$k_{total} = \frac{4Etw^3}{L^3} \tag{2}$$

If the reverse bias voltage is applied across the over-lapping electrode areas, the electrostatic force is given by:

$$F = \frac{A\varepsilon_0 V^2}{2g^2} \tag{3}$$

Where *A* is the overlapping electrode area, ε_0 is the permittivity of free space. *V* is the voltage across the electrodes, *g = (h- d),* h is the initial air-gap thickness, and d is the deflection of the upper electrode toward the lower electrode. Solving above equations for *V* gives:

$$V = (h-d)\sqrt{\frac{L^3 h}{2Etw^3\varepsilon_0 A}} \tag{4}$$

Due to the elastic movement, there is no hysterisis in the wavelength-tuning curve. So, the membrane returns to its original position, where, the voltage is removed. Although increased the air gap leads to a wider tuning range, a larger air gap means a longer cavity length which results in a narrower FSR, and therefore a shorter tuning range. Thus to achieve the maximum tuning range these two parameters must be optimized. The calculated displacement versus voltage for a 150 × 150 µm piston micro mirror with four 100 µm flexures, and a 1.4 µm starting air gap is 470 nm for a 19 volt membrane bias. In this simulation the flexure material is 1.5 µm thick gold (Au) with a Young's modulus of E = 79 GPa. A key feature of this calculation is the expected "snap-down" of top n-DBR which is about 1/3 of the starting air gap.

Coupled thermal equation and rate equation

Dynamic of the VCSELs is primarily governed by the following space and time dependent rate equations coupled with thermal equation as follows (Jungo and Erni, 2003; Samal, 2004):

$$\frac{dN(r,t)}{dt} = \frac{\eta_i J(r,t)}{eV} - \frac{N(r,t)}{\tau_n} + CN^3(r,t) + D_n\nabla^2 N(r,t) - v_g\sum_m G_m(r,t)S_m(t) \tag{5}$$

$$\frac{dS_m(t)}{dt} = \Gamma_m\beta_m\frac{\iint N(r,t)dr}{\pi R^2\tau_n} + \frac{\Gamma_m v_g S_m(t)}{\pi R^2}\iint G_m(r,t)dr - \frac{S_m(t)}{\tau_s} \tag{6}$$

$$C_{th}\frac{dT}{dt} = (P_{el} - P_{opt}) - \frac{T - T'_0}{R_{th}} \tag{7}$$

where *N* is the carrier density, *J* is injection current, η_i is the injection efficiency, τ_n is the carrier recombination lifetime, *V* is the active-region volume, *C* is Auger recombination coefficient, D_n is electron diffusion coefficient, v_g is group velocity, S_m is mth mode the photon density, τ_s is the photon lifetime and β_m is the spontaneous emission coupling coefficient in mth transverse mode, Γ_m is mth mode of optical confinement, R is radius of cavity, P_{opt} and P_{el} are the injected electrical power and generated optical power R_{th} is the thermal resistance of each regions, and C_{th} is thermal capacitance, respectively. G_m is the mth modal gain, which can be approximated as a linear function of the carrier density.

$$G_m(r,t) = g_0\frac{N(r,t) - N_{tr}}{1 + \varepsilon S_m(t)}\left|\Psi_m(r,t)\right|^2 \tag{8}$$

Here g_0 is differential gain, ε is gain compression coefficient and

Table 2. The parameters used in the simulation.

Symbol	Value	Units
η_i	1	
D_n	12	$cm.^2s^{-1}$
β	1.5×10^{-4}	
C	7×10^{-31}	$cm^6.s^{-1}$
τ_s	2.2	ps
τ_n	2.5	ns
N_{tr}	2×10^{18}	cm^{-3}
g_0	1500	cm^{-1}
ε	1.4×10^{-16}	cm^3
N_{th}	5×10^{18}	cm^{-3}
R	12	µm
R_{ox1}	10	µm
R_{ox2}	20	µm
R_{th}	3000	K/W
R_{top}	0.997	
R_{bottom}	0.9985	
P_0	-0.9×10^{7}	
P_1	0.6×10^{-12}	cm^3
P_2	0.25×10^{-14}	$cm^3\ k^{-1}$
P_3	-0.25×10^{26}	cm^{-3}
J_{l0}	7×10^{-4}	kA/cm^2
T_{ref}	139	° k

$|\Psi_m(r,t)|$ is the normalized field amplitude of the *m*th mode. The modification of Equation (5) begins with separation of the time and space variables. This is done for photon density by describing as azimuthal and radial components of the optical field so-called c and s modes (Jungo and Erni, 2003; Samal, 2004):

$$S_m(\rho,\varphi,t) = S_m^c(t)|\Psi_m(\rho)|^2\cos^2(l\varphi) + S_m^s(t)|\Psi_m(\rho)|^2\sin^2(l\varphi) \quad (9)$$

where the index m indicates mode's order and the azimuthal order *l* is a function of *m*. The carrier density profile can be expanded in a time dependent orthogonal series:

$$N(\rho,\varphi,t) = \sum_i N_i(\varphi,t)J_0(\frac{\gamma_i\rho}{R}) = \sum_i J_0(\frac{\gamma_i\rho}{R})\sum_q \left[N_{iq}^c(t)\cos(q\varphi) + N_{iq}^s(t)\sin(q\varphi)\right] \quad (10)$$

Hence, the carrier profile is modelled by describing azimuthal and radial components of the carrier so-called c and s, the carrier profile radial components of the carrier so-called c and s, the carrier profile is expanded in an orthogonal series with time dependent expansion coefficients. Where γ_i is the i^{th} root of the first-order Bessel function of the first kind. The functions is a family of functions with vanishing slope at $\rho=0$ and $\rho=R$ that R is effective cavity radius.The number of required Bessel terms is a function of the effective cavity radius, number of modes, oxide apertures radius, ambipolar diffusion coefficient, and current profile. In this case, 10 terms Bessel series expansion has been taken.

Current confinement and spreading in the cavity is controlled by the size and position of the oxide apertures. Current injection profile engineering in device provides single mode operation. In the structure, smaller aperture is positioned far away from the active region in the p-mirror (R_{ox1}) and a larger aperture is positioned near to the active region in the bottom n-mirror (R_{ox2}). So, the current profile J (ρ, φ, t) can be written as:

$$J(\rho,\varphi,t) = J(t)\rho_c(\rho) \quad (11)$$

where the normalized function $\rho_c(\rho)$ describes the current injection profile, including spreading effects. The electrical model for current injection can be described as:

$$\rho_c(\rho) = 1, \quad \rho \le R_{ox1}$$

$$\rho_c(\rho) = \exp\left[-\frac{(\rho - R_{ox1})^2}{2\gamma^2}\right]$$

$$\gamma = r_s + R_{ox2} \quad (12)$$

Where r_s is the current spreading coefficient.

Small active volume of VCSELs, poor heat dissipation and large resistance introduced by DBRs can exhibit strong thermally dependent behavior. Therefore, for accurate modeling of the device, thermal effects have to be taken into consideration (Jungo and Erni, 2003; Samal, 2004). In our simulations two dominant thermal effects, namely, gain detuning and thermionic emission are considered. Before evaluating these effects, the cavity temperature must be computed. In Equation (8) the dependence of gain on temperature is taken by assuming a parabolic gain spectrum.

$$g_0(\lambda,T) = g_0(1-\frac{T-T_0}{T_{ref}})\left[1-2(\frac{\lambda(T)-\lambda_p(T)}{\Delta\Lambda})^2\right] \quad (13)$$

where T is the cavity temperature, T_0 is the room temperature, T_{ref} is a fitting parameter and $\Delta\Lambda$ is the characteristic width of the parabolic gain approximation. Current leakage due to thermionic emission is also considered as (Jungo and Erni, 2003; Samal, 2004):

$$J_l(N,T) = J_{l0}\exp(-\frac{p_0}{T} + \frac{P_1N}{T} + P_2N + \frac{P_3}{T(N+N_{th})}) \quad (14)$$

J_{l0} is reference leakage current density and P_0, P_1, P_2 and P_3 are leakage parameters. The numerical values of parameters are summarized in Table 2.

RESULTS AND DISCUSSION

To enhance the performance of MEMS-VCSEL, we propose two new structures with n-aperture fixed at the first mirror-pair of the n-DBR whose size is twice the diameter of the p-aperture. In the first structure (new structure-1) the p-aperture is placed in the first mirror-pair of the p-DBR, in the second structure (new structure-2) the p-aperture is placed in the third mirror-pair of the p-DBR as compared with conventional VCSEL (with a 5 µm single oxide aperture in bottom n-DBR). Spatial-current distribution versus radius distance of conventional VCSEL and the proposed structures are shown in Figure 2.

The relative size and location of the dual asymmetric

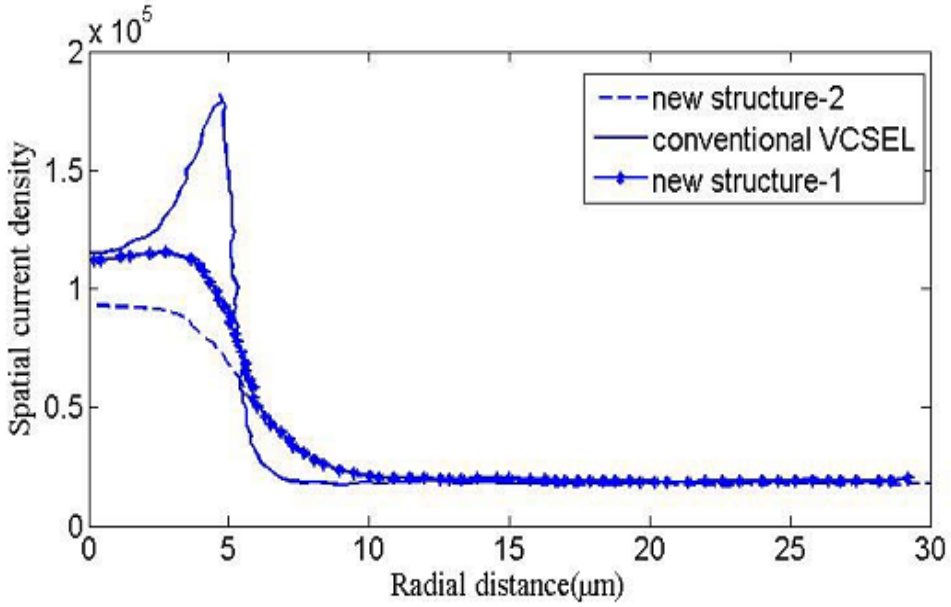

Figure 2. Spatial-current distribution vs. radial distance in conventional (solid), New structure-1(star dash) and new structure-2 (dash).

oxide apertures and doping profiles of the DBR mirrors, affect the shape of spatial injection current profile in active region. The spatial current density distribution shows a ring shape injection profile for a conventional VCSEL with a maximum at the periphery and a minimum at the center of the device. The new structure-1 and new structure-2 show an improvement in the profile over the conventional structure when the p-aperture is moved farther away from the active region. The new designs show bell shape injection profiles, which make them suitable for single mode operation. A bell shape current injection profile is favourable for a LP01 mode of a VCSEL laser. However, the new structure-2 shows a better performance for single mode operation and we use this structure in our simulations.

The steady-state output power is shown in Figure 3. Because of higher leakage current and gain detuning in conventional VCSEL, the thermal rollover appears above 10 mA compared with new structure which occurs at 15 mA. It can be seen that new structure has lower temperature rise versus conventional structure. This MEMS-VCSEL can be less temperature sensitive than conventional VCSEL. In addition, for a constant injection current the temperature difference goes to zero far from the VCSEL center. This lower temperature sensitivity enables us to stabilize the emission wavelength of a tunable VCSEL within one nanometer over a broad range of operation temperature.

3D distribution of carrier density and photon intensity for conventional and the new structures are shown in Figure 4a and b. The conventional structure exhibits several higher order modes, but the single mode operation of the new structure is evident in Figure 4b. Figures show the dominant modes for conventional and new structure designs. The conventional design shows LP41 is the most dominant mode and the fundamental LP01 mode more than 40 dB lower than the dominant mode. New structure design shows LP01 as the dominant mode with the next higher mode more than 40 dB lower in this case.

The large signal responses of devices are compared in Figure 5. Calculated results show multi transverse modes operation for conventional VCSEL and high power output with dominant LP01 mode in the new structure. Tuning range of 40 nm for a 19 volt membrane bias is shown in Figure 6. The continuous repeatable and hysteresis-free tuning range can be observed clearly, which makes it suitable for DWDM systems.

Conclusions

We have designed a novel MEMS-VCSEL with asymmetric double oxide aperture and highly strained GaInNAsSb GaNAs quantum wells for DWDM optical communication systems. We have demonstrated a comprehensive model including electrostatic membrane equation coupled with thermal, spatial and temporal rate equations considering SRH, Auger and carrier diffusion effects. The coupled equations are solved numerically using FDM to find self-consistent solutions for tunable, single mode and high power of operation. The electrically-pumped MEMS-VCSEL can be directly modulated with wide tuning range. We have illustrated

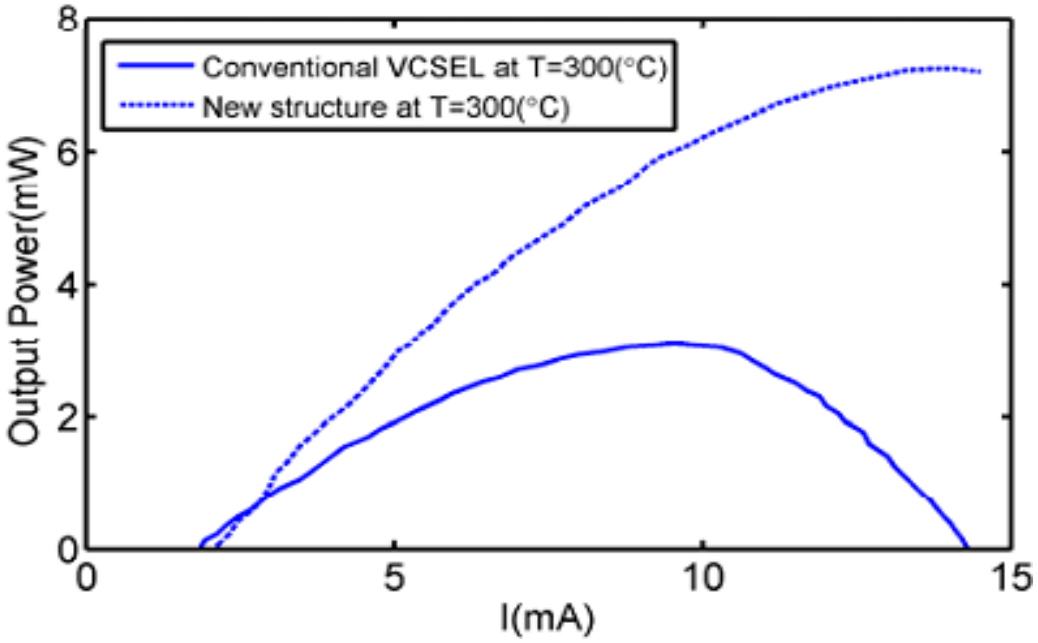

Figure 3. Thermal rollover in the new structure and conventional design at room temperature.

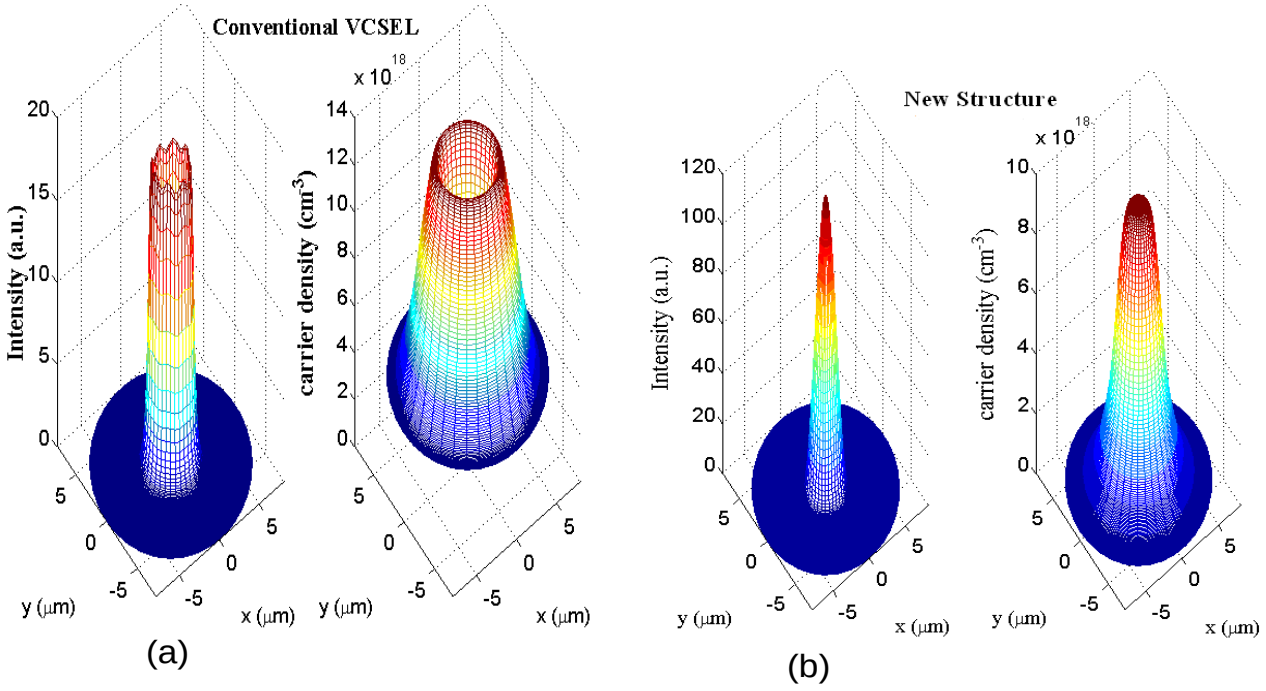

Figure 4. Carrier density and photon intensity of (a) conventional design and (b) new structure.

the large and small signal response of new structure with 40 nm tuning range. Single mode operation is achieved by asymmetric double oxide apertures. The thermal effects as gain detuning and carrier leakage are investigated. The new structure design, demonstrated a room temperature CW single-mode output power of more than 7 mW with a side mode suppression ratio greater than 25 dB for an active device size more than 12 μm in

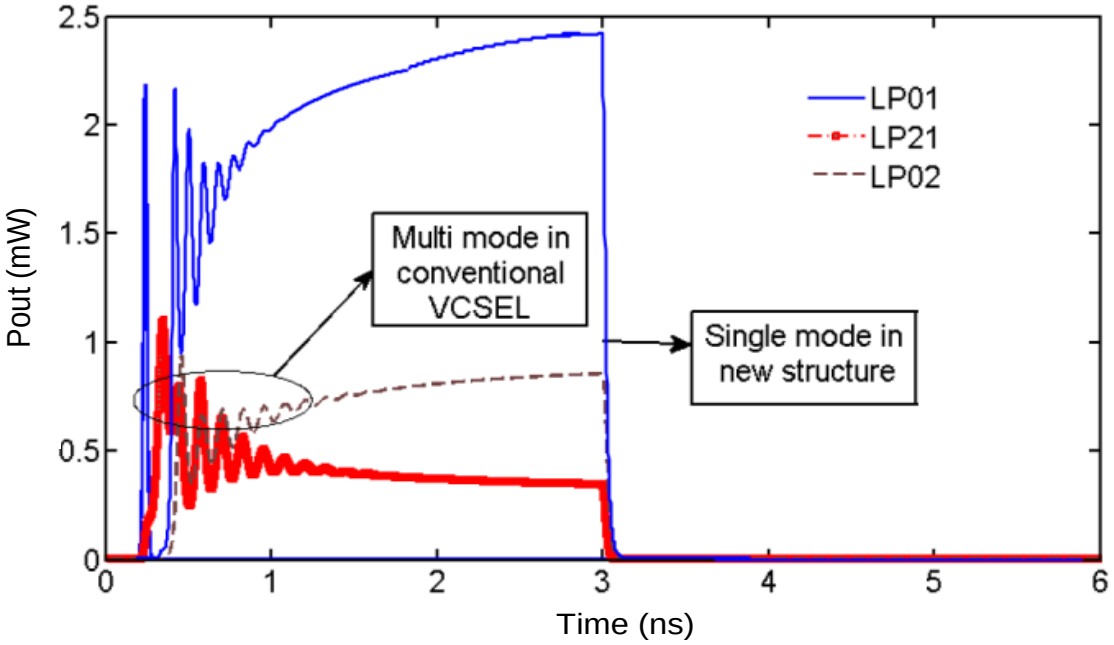

Figure 5. Small signal response in conventional (solid) and the new structure (dash).

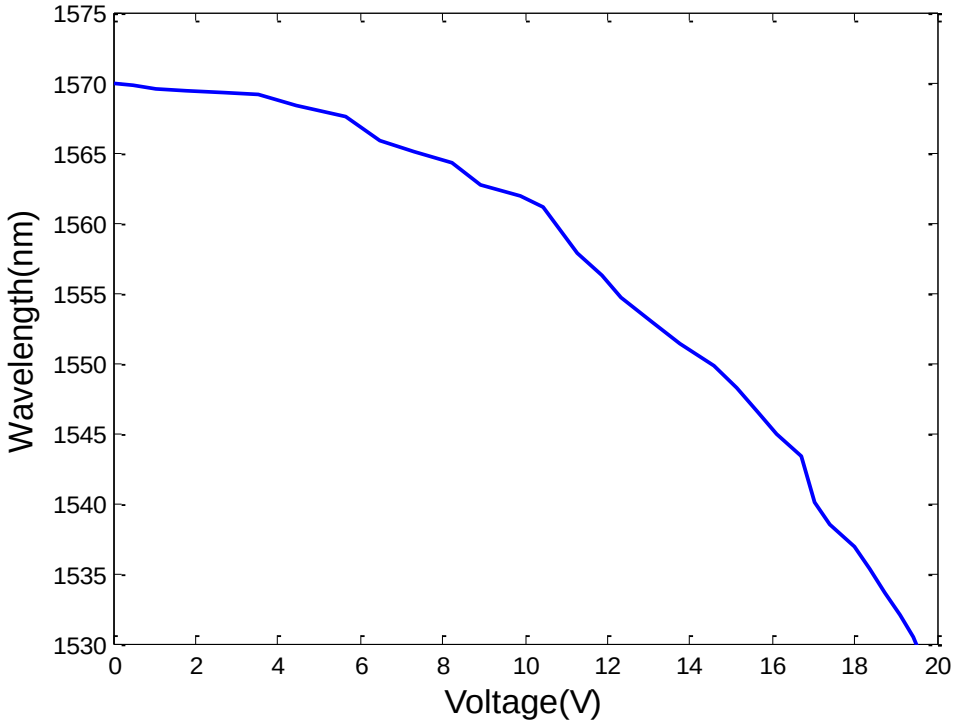

Figure 6. Tuning range in the new structure.

radius. It has been shown that thermal rollover occurs at higher injection current as compared to with conventional VCSEL.

REFERENCES

Chang-Hasnain CJ (2000). Tunable VCSEL. IEEE J. Selected Topic Quantum Elect. 6:978-987.

Guan B, Guo X, Deng J, Shen G (2009). Investigation on Tunable Wavelength and Modal Characteristics of MEMS Tunable Vertical Cavity Surface Emitting Lasers, Asia Communications and Photonics Conference and Exhibition (ACP), China.
Gutowski K, Sarzala RP (2008). Computer simulation of tuned and detuned GaInNAsSb QW VCSELs, Mate. Sci. Poland. pp. 26-45.
Jungo M, Erni D (2003). VISTAS: A Comprehensive System Oriented Spatio temporal VCSEL Model. IEEE J. Selected Topics Quantum Elect. 9(3):939-948.
Kogel B, Debernardi P, Westberg P, Haglund A, Gustavsson J, Bengtsson J, Haglund E, Larsson A (2011). Single mode tunable VCSELs with integrated MEMS technology, Proceedings of the European Conference on Laser and Electro-Optics (CLEO/Europe), Paper CB8.5-WED. Germany.
Martin WA (2001). Micro machined Tunable VCSELs for Wavelength-Division Multiplexing Systems, Ph.D. Thesis, Stanford University.
Nakwaski W, Sarzala R (1998). Transverse-Modes Control of Vertical-Cavity Surface-Emitting Lasers. Opt. Commun. 148:63-69.
Ochoa EM (2007). Hybrid Micro Electro Mechanical Tunable Filter Ph.D. Thesis, Air Force Institute of Technology University.
Samal N (2004). Ph.D. Thesis, High-power Single-mode Vertical Cavity Surface Emitting Lasers, Arizona State University.
Samal N, Johnson SR, Ding D (2005). High-power Single-mode Vertical-Cavity Surface-Emitting Lasers. J. Appl. Phys. Lett. 87(22):161108-161124.
Tayebati P, Wang P, Azimi M, Maflah L, Vakhshoori D (1999). Half-Symmetric Cavity Micro electro mechanically Tunable Vertical Cavity Surface Emitting Lasers with Single Spatial Mode Operating Near 950 nm. IEEE Photon. Technol. Lett. 75(7):897-898.
Zhou D, Mawst LJ (2002). High-power single-mode anti resonant reflecting optical waveguide-type vertical-cavity surface-emitting lasers. IEEE J. Quantum. 38:1599-1606.